J Appl Electrochem (2007) 37:567–573
DOI 10.1007/s10800-006-9286-9

ORIGINAL PAPER

Synthesis and electrochemical evaluation of carbon coated Cu_6Sn_5 alloy-graphite composite lithium battery anodes

N. Jayaprakash · N. Kalaiselvi · C. H. Doh

Received: 9 February 2006 / Accepted: 11 December 2006 / Published online: 13 January 2007

Abstract With a view to minimize the unavoidable large volume changes of tin based Cu_6Sn_5 alloy anodes, a composite Cu_6Sn_5/graphite anode has been prepared via. a mechanical alloying process and subsequently coated with disordered carbon through pyrolysis of PVC. Phase pure products with better crystallinity and preferred surface morphology were obtained, as evident from PXRD and SEM respectively. Upon electrochemical charge-discharge, the intermetallic Cu_6Sn_5 alloy-graphite composite anode was found to exhibit an enhanced initial discharge capacity of 564 mAh g^{-1} followed by significant capacity fade (>20%) especially after five cycles. On the other hand, carbon coated Cu_6Sn_5 alloy-graphite composite demonstrated promising electrochemical properties such as steady reversible capacity (~200 mAh g^{-1}), excellent cycle performance (<5% capacity fade) and high coulombic efficiency (~98%) via. significant reduction of volume changes. The carbon coating offers buffering and conductive actions on the anode active material and thereby enhances the electrochemical behavior of carbon coated Cu_6Sn_5 alloy/graphite composite anode material.

Keywords Carbon coated Cu_6Sn_5 alloy-graphite composite anode · Lithium battery · Specific capacity · Coulombic efficiency

N. Jayaprakash · N. Kalaiselvi (✉)
Central Electrochemical Research Institute,
Karaikudi 630 006, India
e-mail: kalakanth2@yahoo.com

C. H. Doh
Korea Electrotechnology Research Institute,
Changwon 641 600, South Korea

1 Introduction

Despite the improved capacity of carbonaceous anode materials and the demonstrated higher specific capacity values [1–5], development of next generation lithium-ion batteries requires exploration of alternate electrode materials to increase the specific energy. As far as alternative anode candidates are concerned, transition metal oxides [6–8], metal–metal alloys [9–11], transition metal vanadates [10], ATCO anodes [11, 12], metalloids [13] and a variety of lithium metal oxides such as $LiMSnO_4$ [14], phosphates [15], niobates [16] and ferrites [17–22] have been examined. Tin based anode materials with a theoretical capacity of 994 mAh g^{-1} corresponding to the formation of $Li_{4.4}Sn$ are receiving a great deal of attention as better candidates in place of graphite (372 mAh g^{-1}). Basically, mechanical decrepitation problems related to tin anodes hamper their wider acceptance in practical lithium battery applications. As a result, tin based alloy/composite anodes with a special reference to Fe–Sn type intermetallic alloys [23] have gained importance. Further, the recent announcement of Fuji's amorphous tin composite oxide (TCO) anodes [24] has generated renewed recognition to Sn based alloy/composite anodes.

Among the various alloy combinations, Cu_6Sn_5 has lower capacity fade, as the copper matrix partially reduces problems associated with the expansion and contraction of Li_xSn alloys on cycling: i.e., it is anticipated that extensive lithiation of Cu_6Sn_5 anodes would initially result in a breakdown of the parent compound to form copper [inactive component] and tin [active component], from which tin provides the anode capacity and the copper, dispersed in the solid, acts as

an electronically conducting matrix to mitigate some of the undesired volume changes observed with the alloy anode. Therefore, with a view to obtaining reasonably good capacity values with little capacity fade, Cu_6Sn_5 anodes were chosen as the parent material for the present study.

The concept of using an inert matrix to shield a battery anode, which was proposed by Huggins et al. [25], and examined further by Besenhard [26–28], Kepler [29] and Yang et al. [30] produces enhanced specific capacity and cycle performance of encapsulated tin based anodes. Similarly, there have been attempts to form graphite anodes doped with tin [31], wherein tin boosts the capacity of graphite. In contrast, tin based alloy (Cu_6Sn_5), as the main active phase combined with graphite to provide structural support, has been prepared via. ball milling in the current study.

Based on earlier extensive studies on Sn based alloys, it is strongly believed that improving the dimensional stability of alloy/composite anodes during Li insertion/extraction cycling is a vital factor required to realize better cycling performance [29]. A new strategy to address this issue is to uniformly coat a carbonaceous material over the surface of an alloy composite anode. Such an attempt has been made in the present investigation by preparing carbon coated Cu_6Sn_5-graphite composite powder.

Thus, the main focus of this paper is to explore the possibility of achieving synergistic effects of the high lithium storage capacity of Sn and the cyclability of graphite in one system, viz., graphite coated Cu_6Sn_5 and to realize the added beneficial effects of buffering and the conductive nature of carbon through the carbon coated Cu_6Sn_5/graphite composite anode material. In this regard, the present study deals with the synthesis, characterization and electrochemical performance of Cu_6Sn_5/graphite composite and carbon coated Cu_6Sn_5-graphite composite anodes against lithium metal.

2 Experimental

2.1 Synthesis procedure

Figure 1 shows a schematic representation of the formation of Cu_6Sn_5 alloy, Cu_6Sn_5 alloy/graphite composite and the coating process on the alloy-graphite matrix. An easy-to-adopt mechanical alloying method was used to synthesize the parent Cu_6Sn_5 alloy and alloy/graphite composite anodes. On the other hand, carbon coating was carried out through the pyrolysis of PVC, a polymer with no oxygen content, in order to

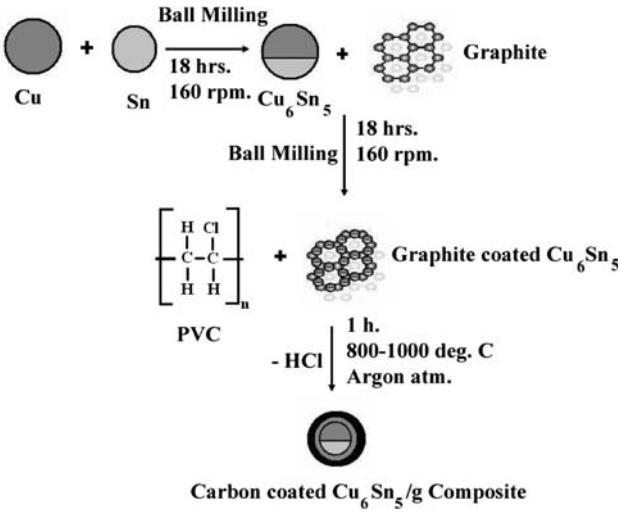

Fig. 1 Schematic representation of Carbon coating on Cu_6Sn_5/graphite composite

avoid the risk of tin oxidation upon decomposition of the polymer, which is the highlight of this study. Even though it is reported that carbon coating through propylene carbonate based electrolyte reduces the irreversible capacity of anodes [32], disordered carbon coating through the pyrolysis of PVC has been chosen for this study, based on the fact that porous PVC polymer absorbs the alloy/graphite composite precursor effectively [33].

Analytical grade powders of tin and copper (99.9%pure, Sigma Aldrich, South Korea) were taken in the ratio of 5:6 in a container with zirconium balls of two different sizes (in the ratio 2:4) to ensure complete milling and to yield sub micron sized particles. The container was air sealed with paraffin films to prevent entry of atmospheric air, which might lead to the oxidation of the alloy material. Subsequently, Argon gas was passed into the container at a constant rate for 30 min to flush out the residual air. Then the Argon filled container was fixed into the ball mill and allowed to run for 60 h at 120 revolutions per minute. The as milled fine alloy powder was taken out and sieved with grinding for equal particle size distribution.

2.2 Graphite coating

The ball milled Cu_6Sn_5 alloy sample was mixed with graphite (Dag-68, Sodiff, 1:1 ratio) and was subjected to ball milling for 18 h at 160 revolutions per minute in a planetary ball mill in the same manner as mentioned above. The Cu_6Sn_5/graphite composite material thus

obtained was taken out, sieved and subjected to characterization studies.

2.3 Carbon coating

Finally, carbon coating to the alloy-graphite composite was carried out by mixing the Cu_6Sn_5/graphite composite with 70 wt.% PVC in a mortar and heating the mixture at 800–1000 °C under argon flow for one hour in an alumina heating boat. The heating rate was 10 °C per minute and the sample was taken out and ground further to obtain ultra fine powders of carbon coated Cu_6Sn_5/graphite composite.

2.4 Physical and electrochemical characterization

Phase characterization was done by powder X-ray diffraction on a Philips 1830 X-ray diffractometer using Ni filtered Cu-Kα radiation (λ = 1.5406) in the 2θ range 10–120° at a scan rate of 0.04° s^{-1}. Surface morphology of the particles was examined through SEM images obtained from Jeol S-300 H Scanning Electron Microscope. The actual size of the particles was measured using a Malvern Easy Particle Size Analyzer and charge discharge studies were carried out using MACCOR charge-discharge cycler.

2.5 Electrode preparation and coin cell fabrication

Electrochemical charge-discharge evaluation was carried out on 2016 coin cells fabricated using the synthesized anodes and Li metal. The electrodes were made by dispersing 90 wt.% of active material and 10 wt.% of poly (vinyldene fluoride) (PVDF) binder in *N*-methyl-2pyrrolidone (NMP) solvent. The resulting slurry was spread on a copper foil, dried for 12 h to remove the excess NMP and then hot roll pressed into sheets. 2016 coin cells were fabricated with the electrodes punched out from the sheet and lithium was used as the counter electrode. EC/DMC/EMC/PC (4/3/3/1 by vol.) dissolved in 1.0 M $LiPF_6$ (Cheil Industries Ltd, South Korea) electrolyte and an Asaki polypropylene separator were used.

3 Results and discussion

3.1 Phase formation results—XRD analysis

The presence of broad and well-defined peaks at 2θ = 29 & 42°, is the striking evidence for the formation of size controlled Cu_6Sn_5 alloy particles (Fig. 2a).

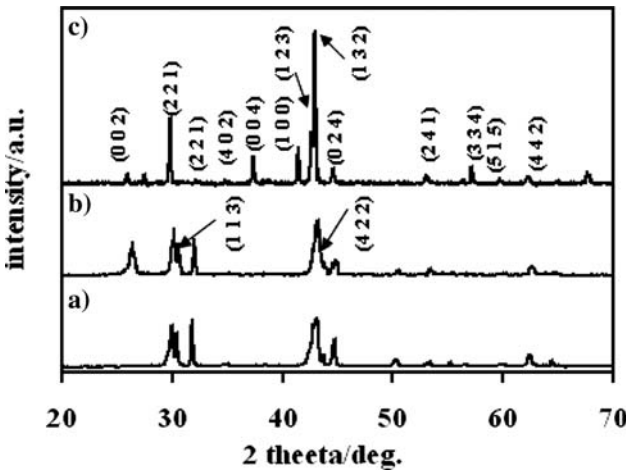

Fig. 2 XRD pattern of alloy composite material (**a**) Cu_6Sn_5 alloy, (**b**) Cu_6Sn_5/graphite composite, and (**c**) Carbon coated Cu_6Sn_5/graphite composite

Similarly, the Cu_6Sn_5 alloy/graphite composite obtained after 18 h ball milling also exhibited broader peaks, as evident from Fig. 2b. This may be attributed to the prolonged and high-speed ball milling process that has played a vital role against particle agglomeration. In other words, ball milled Cu_6Sn_5 alloy/graphite composite powders also have smaller particle size, well within the desired micron level. On the other hand, carbonization of PVC above 500 °C is found to slightly increase the crystalline size [discussed in the particle size analysis section], despite the monotonic decrease of the h/c atomic ratio especially at 1000 °C [33]. As a result, the carbon coated over the alloy/graphite composite is expected to have disordered or amorphous nature, as reported by Lee et al. [32]. However, the disordered carbon is found to wrap and mask the entire surface of Cu_6Sn_5/graphite composite due to which the peak corresponding to graphite, which is obvious at 2θ = 26° (Fig. 2b), is not visible in the carbon coated alloy graphite composite powder (Fig. 2c).

Similarly, the (004) diffraction peak of graphite at 2θ = 56° is reported to be indistinguishable [34] and the same is realized with the present set of graphite/carbon coated alloy composite powders. Based on the restricted broadening of Bragg peaks observed for the native Cu_6Sn_5 and the Cu_6Sn_5/graphite composite powders (Fig. 2a, b), it is understood that the process of ball milling is found to be effective in controlling the size of the individual particles to some extent. On the other hand, the process of pyrolysis at high calcination temperature does not seem to have any significant control against the growth of particles. It is obvious from the Fig. 2c that unlike the previous samples (Fig. 2a, b), narrow peaks were exhibited by the carbon

coated Cu_6Sn_5 alloy/graphite composite anode powder, which is an indication for the possible presence of size grown particles due to the high temperature (1000 °C) treatment.

3.2 Morphological results—SEM and particle size analysis

The Scanning Electron Microscopic images of the as ball milled alloy, Cu_6Sn_5 alloy/graphite composite and the carbon coated Cu_6Sn_5/graphite composite are shown in Fig. 3a–c. The presence of spherical grains with definite grain boundaries and the uniform distribution of graphite/coating of carbon over the surface of Cu_6Sn_5 alloy are obvious from Fig. 3b, c. The perfect masking of the encapsulated Cu_6Sn_5/graphite composite matrix via. tight wrapping of the amorphous carbon layer is clearly seen in Fig. 3c.

An average particle size distribution of 4–9 μm was found with the present set of compounds, which is further confirmed from the particle size analysis of the individual compounds. The size of the native Cu_6Sn_5 alloy particles was measured as 4.8 μm, which upon treatment with graphite slightly increased to 5.6 μm (Fig. 4a, b). Therefore, as mentioned in the PXRD results, the process of ball milling has some effect over the size control of mechanically alloyed Cu_6Sn_5/graphite composite particles against particle agglomeration. However, further coating of carbon over Cu_6Sn_5/graphite composite prepared via. pyrolysis of PVC at 1000 °C was found to enhance the size of the particles to 8.9° μm (Fig. 4c), which is almost twice the size of the parent alloy powder (Fig. 4a). This increased particle size is an indication of chunky deposition of amorphous carbon particles over Cu_6Sn_5/graphite composite, thus responsible for the complete masking of encapsulated alloy/graphite matrix. This is further substantiated by the presence of sharp peaks observed in the PXRD pattern of carbon coated Cu_6Sn_5/graphite composite material, as previously discussed.

3.3 Charge-discharge behavior

Generally, tin based anodes with larger particle size pulverize rapidly during charge-discharge cycle due to volume mismatch, resulting in a rapid drop in reversible capacity upon cycling. However, this pulverization will be less extensive with respect to smaller [micron/sub-micron sized] particles, because the micron-sized cavities within the powder can absorb the expansion of

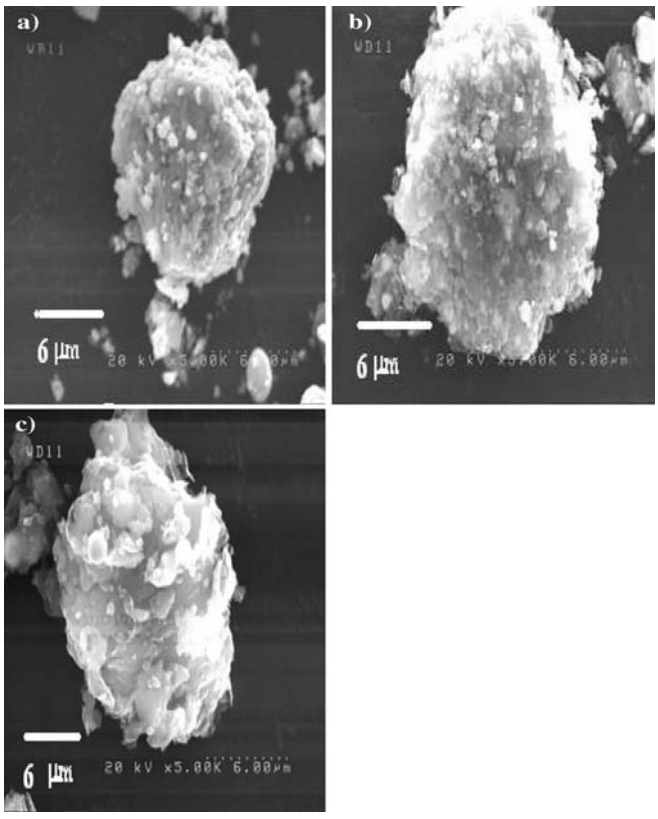

Fig. 3 Scanning Electron Microscopic images of the composite material (**a**) Cu_6Sn_5 alloy, (**b**) Cu_6Sn_5/graphite composite, and (**c**) Carbon coated Cu_6Sn_5/graphite composite

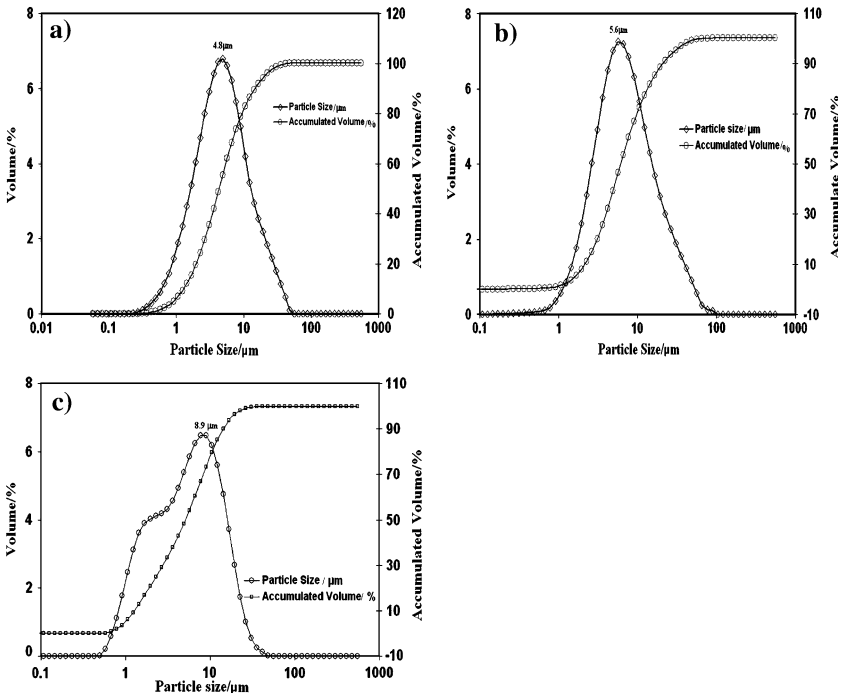

Fig. 4 Particle size distribution plot of the composite material (**a**) Cu_6Sn_5 alloy, (**b**) Cu_6Sn_5/graphite composite, and (**c**) Carbon coated Cu_6Sn_5/graphite composite

materials during the formation of lithium compounds [33]. Therefore, it is postulated that size reduced particles of the electrodes may reduce the extent of pulverization and thereby enhance the electrochemical behavior upon cycling. Based on the micron size particles (<10 μm) present in the Cu_6Sn_5/graphite composite and carbon coated Cu_6Sn_5/graphite anode powders, it is expected that the anodes prepared in the present study would exhibit improved electrochemical performance in rechargeable lithium batteries.

The electrochemical performance of Cu_6Sn_5/graphite composite and carbon coated Cu_6Sn_5/graphite composite anodes was measured by deploying them individually as working electrodes against a lithium metal counter electrode under C/10 rate charge-discharge conditions. The first discharge capacity of Cu_6Sn_5/graphite and carbon coated graphite/alloy composite anodes were found to be 564 and 303 mAh g^{-1}, respectively [Fig. 5a]. When the Cu_6Sn_5 alloy is encapsulated in a graphite structure, the ductile graphite acts as a buffer layer to absorb volume expansion due to Li_xSn alloy formation, and enhances the electrochemical behavior of the Cu_6Sn_5/graphite composite. As expected, the addition of graphite to the Cu_6Sn_5 alloy enhanced the specific capacity values of the first few cycles (564–520 mAh g^{-1}) and reduced the irreversible capacity values significantly, but the same behavior was not found to be maintained upon cycling. In other words, an increased initial capacity of about 520~560 mAh g^{-1} has been observed, which may be

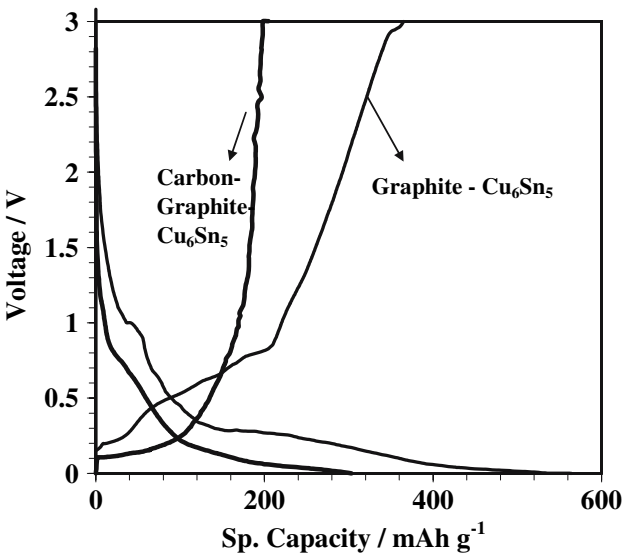

Fig. 5 Charge-discharge behavior of Cu_6Sn_5/graphite composite and the carbon coated Cu_6Sn_5/graphite composite

due to the initial electrochemical grinding of alloy/graphite composite particles. Then, the specific capacity (~300 mAh g^{-1}) faded gradually up to 10 cycles (~40%) and further decreased to the extent of about 150 mAh g^{-1} within 20 cycles (~70%). This observation is not unusual, as it is similar to that reported by Tamura et al. [34], wherein the electrodeposited tin based alloy without heat treatment experiences such capacity fade problems upon cycling, irrespective of the improved initial specific capacity values. So, the

observed higher initial specific capacity value of Cu_6Sn_5/graphite composite may be attributed to the uniform distribution of graphite particles over the alloy matrix which is responsible for the significant reduction of volume changes, via. buffering action. Further, the incorporation of graphite could facilitate easy insertion/extraction of Li through the vacancies, micro cavities and voids of the alloy matrix [35], but not effectively for a longer period. Hence, the fade in capacity after five cycles becomes unavoidable.

In addition, it is presumed that the addition of graphite decreases the extent of swelling of active material during the reaction with lithium and thereby decreases the reactivity of the active material with the electrolyte simultaneously. Similarly, the process of ball milling has not resulted in a significant reduction in particle size to an extent of well below 1 μm and so the actual surface area exposed to the electrolyte is not enhanced. As a result, the magnitude of initial irreversible capacity loss could be minimized reasonably in the Cu_6Sn_5/graphite composite [Fig. 6a], along with the gradually enhancing coulombic efficiency values (65–95%), despite the unavoidable capacity fade observed upon cycling.

On the other hand, the carbon coated alloy/graphite composite anode exhibits excellent coulombic efficiency values, even upon extended cycling, irrespective of the slightly reduced initial specific capacity values. This behavior is an indication that the treatment of carbon coating has improved the conductive contact between the M_1–M_2 (Cu_6Sn_5) alloy and the graphite particles along with surface modification, which enhances the capacity retention behavior upon progressive cycling.

Similarly to the reported efforts to improve the interface strength between electrode active material and current collector through post-heat treatment [34], the present study also deals with the pyrolysis of PVC to introduce carbon coating on the mechanically alloyed Cu_6Sn_5/graphite composite matrix. As a result, the capacity retention capability has risen from 62 to 82% in the second cycle and thereafter to 98%, which is a remarkable improvement (Fig. 6b). This improvement in capacity retention and maintenance of structural stability upon cycling (Fig. 6b) may result from enhanced interface strength between the whole of the active material and the current collector. Stress on the interfaces between the layers of Cu_6Sn_5 alloy is decreased due to the pyrolysed disordered carbon coating on the surface of the composite matrix. As a result, the separation of active material from the interface of each layer is suppressed. Thus carbon coating controls the fining of entire active material, its reaction with the electrolytes and the decrease in electronic conductivity among the active material and the current collector so that the cycling performance is improved [34].

Thus, it is very well demonstrated through the present study that the specific capacity values and initial cycling performance of native Cu_6Sn_5 alloy may be improved and that further improvement in terms of high coulombic efficiency (>95%) with excellent cycling stability would be possible via. carbon coating. Thus, graphite imparts a buffering action on the Cu_6Sn_5 alloy and the carbon coating improves both the conductive and buffering activities of the Cu_6Sn_5 anode matrix.

4 Conclusion

Cu_6Sn_5 alloy and Cu_6Sn_5/graphite composite anode powders were synthesized via. ball-milled solid state fusion of precursors and the subsequent carbon coating was carried out through pyrolysis of PVC at 100 °C. A slight increase in the size of mechanically alloyed Cu_6Sn_5/graphite particles was observed (4.8~5.6 μm) and the increase in particle size was found to be significant in the case of pyrolysed carbon coated Cu_6Sn_5/graphite composite powders (8.9 μm). When deployed as anodes in rechargeable lithium batteries, the anode

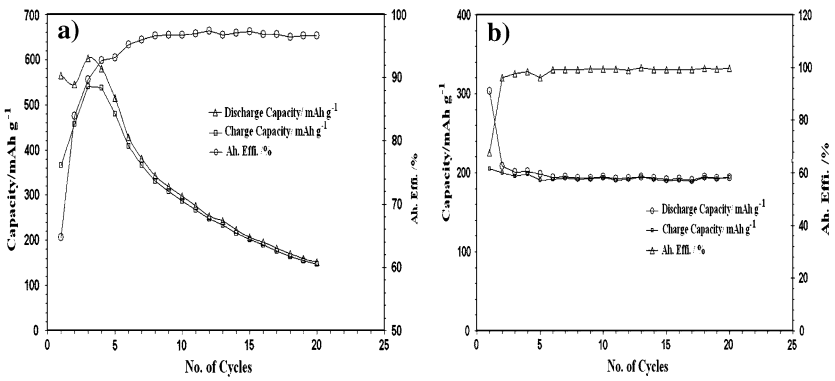

Fig. 6 Capacity vs cyclability behavior of (**a**) Cu_6Sn_5/graphite composite and (**b**) Carbon coated Cu_6Sn_5/graphite composite

exhibited a maximum capacity of ~564 mAh g^{-1} against 303 mAh g^{-1}, shown by carbon coated alloy/graphite composite. Hence, graphite coating is effective in enhancing the initial specific capacity of native Cu_6Sn_5 alloy anodes. However, carbon coating on Cu_6Sn_5 alloy-graphite composite was found to be advantageous, especially ameliorate volume changes by enhancing the columbic efficiency [98%] of the Cu_6Sn_5 anode upon extended cycling via. synergetically improved buffering and conductive actions on the native Cu_6Sn_5 anode material.

References

1. Claye A, Fisher JE (1999) Electrochim Acta 45:107
2. Sato K, Noguchi M, Demachi A, Oki N, Endo M (1994) Science 264:556
3. Dahn JR, Zheng T, Liu Y, Xue JS (1995) Science 270:590
4. Zheng T, Liu Y, Fuller EW, Tseng S, Von Sacken U, Dahn JR (1995) J Electrochem Soc 142:2581
5. Han Y-S, Yu J-S, Park G-S, Lee J-Y (1999) J Electrochem Soc 146:3999
6. Cheng X-Q, Shi P-F (2005) J Alloys Compd 391:241
7. Reddy MV, Wannek C, Pecquenard B (2003) J Power Sources 119–121:101
8. Choi SH, Kim JS, Yoon YS (2004) Electrochim Acta 50:545
9. Idota Y, Kubota T, Matsufuji A, Miyasaka T (1997) Science 276:1395
10. Nishijma M, Takeda Y, Imanishi N, Yamamota O (1994) J Solid State Chem 113:205
11. Satya Kishore MVVM, Varadaraju UV, Raveau B (2004) J Solid State Chem 77:3981
12. Kalaiselvi N, Doh C-H, Park C-W, Moon S-I, Yun M-S (2004) Electrochem Commun 6:1110
13. Son JT (2004) Electrochem. Commun 6:990
14. Chu Y-Q, Fu Z-W, Qin Q-Z (2004) Electrochim Acta 49:4915
15. Yang X, Wang X, Zhang Z (2005) J Crystal Growth 277:463
16. Alcántara R, Jaraba M, Lavela P, Tirado JL, Jumas JC, Olivier-Fourcade J (2003) Electrochem Commun 5:16
17. NuLi Y-N, Qin Q-Z (2005) J Power Sources 142:292
18. NuLi Y-N, Chu Y-Q, Qin Q-Z (2004) J Electrochem Soc 151:A1077
19. Sharma N, Shaju KM, Subba Rao GV, Chowdari BVR (2003) J Power Sources 124:204
20. Ahn H-J, Choi H-C, Park K-W, Kim S-B, Sung Y-E (2004) J Phys Chem B 108:9815
21. Fan J, Wang T, Fu C, Tu B, Jiang Z, Zhao D (2004) Adv Mater 16:1432
22. Wang Y, Lee JY, Chen B-H (2004) J Electrochem Soc 151:A563
23. Mao O, Turner RL, Countney IA, Fredericksen BD, Buckett MI, Krause LJ, Dahn JR (1999) Electrochem Solid State Lett 2:3
24. Idota Y, Kubota T, Matsufuji A, Mackawa Y, Miyasaka T (1997) Science 276:1395
25. Wang J, Raistrick ID, Huggins RA (1986) J Electrochem Soc 133:457
26. Besenhard JO, Komenda P, Paxinos A, Wudy E, Josowicz M (1986) Solid State Ionics 18–19:823
27. Besenhard JO, Hess M, Komenda P (1990) Solid State Ionics 40–41:525
28. Besenhard JO, Yang J, Winter M (1997) J Power Sources 68:87
29. Kepler KD, Vaughey JT, Thakeray MM (1999) J Power Sources 81–82:383
30. Yang J, Winter M, Besenhard JO (1996) Solid State Ionics 90:281
31. Wang GX, Ahn JH, Lindsay MJ, Sun L, Broadhurst DH, Dou SX, Liu HK (2001) J Power Sources 97–98:211
32. Lee HY, Back JK, Jang SW, Lee SM, Hong ST, Lee KY, Kim MH (2001) J Power Sources 101:206
33. Patel P, Kim IS, Maranchi J, Kumta P (2004) J Power Sources 135:273
34. Tamura N, Ohshita R, Fujimoto M, Fujitani S, Kamino M, Yonezu I (2002) J Power Sources 107:48
35. Mabuchi A, Tokumilsu K, Fujimoto H, Kasch T (1995) J Electrochem Soc 142:1041